Information Processing in Agriculture 12 (2025) 40–53

Contents lists available at ScienceDirect

Information Processing in Agriculture

journal homepage: www.keaipublishing.com/en/journals/information-processing-in-agriculture/

An automatic method for estimating insect defoliation with visual highlights of consumed leaf tissue regions

Gabriel S. Vieira [a,b,*], Afonso U. Fonseca [b], Naiane Maria de Sousa [b], Julio C. Ferreira [a], Juliana Paula Felix [b], Christian Dias Cabacinha [c], Fabrizzio Soares [b]

[a] Federal Institute Goiano, Computer Vision Laboratory, Urutaí GO, Brazil
[b] Federal University of Goiás, Pixellab Laboratory, Goiânia GO, Brazil
[c] Federal University of Minas Gerais/UFMG, Institute of Agrarian Science, Montes Claros MG, Brazil

ARTICLE INFO

Keywords:
Leaf area measurement
Defoliation
Insect predating
Smart farming
Precision agriculture

ABSTRACT

As an essential component of the architecture of a plant, leaves are crucial to sustaining decision-making in cultivars and effectively support agricultural processes. When the leaf area is constantly monitored, a plant's health and productive capacity can be assessed to foment proactive and reactive strategies. Because of that, one of the most critical tasks in agricultural processes is estimating foliar damage. In this sense, we present an automatic method to estimate leaf stress caused by insect herbivory, including damage in border regions. As a novelty, we present a method with well-defined processing steps suitable for numerical analysis and visual inspection of defoliation severity. We describe the proposed method and evaluate its performance concerning 12 different plant species. Experimental results show high assertiveness in estimating leaf area loss with a concordance correlation coefficient of 0.98 for grape, soybean, potato, and strawberry leaves. A classic pattern recognition approach, named template matching, is at the core of the method whose performance is compared to cutting-edge techniques. Results demonstrated that the method achieves foliar damage quantification with precision comparable to deep learning models. The code prepared by the authors is publicly available.

1. Introduction

Inspecting and controlling agricultural activities is essential to ensure quality and production rates according to the planting estimates [1]. However, several variables must be observed, and the indicators must be reliable to support agricultural management and decision-making [2]. Monitoring insects in plantations is equally important to observe the potential damage caused by chewing and cutting insects. In a balanced ecosystem, the coexistence between plants and insects can be beneficial, as in the increase in the concentration of nutrients and water in the soil (e.g., anthills), or acceptable when production is little affected [3]. However, it is estimated that insects consume about 14% of the total global agricultural production, and without proper control, they can bring several losses [4]. Therefore, the threshold level of 30% defoliation in the leaf growth phase (vegetative stage) or 15% in the grain formation phase (reproductive stage) is still considered valid for the control of defoliating caterpillars in soybean [5].

Different methods have assisted in defoliation estimation. Traditional approaches use manual measurement instruments and can be assertive. However, they depend on operator experience, have cost and operational effort relative to the number of samples for analysis, and are susceptible to human subjectivity. Approaches that use leaf area measuring equipment support more significant amounts of image samples but are expensive and require maintenance and calibration. Computer-based approaches can handle more extensive image databases, reduce subjectivity, provide quick responses, and be cheaper than other approaches. Nevertheless, some solutions do not support defoliation estimation with leaf edge damage, require user interaction, or rely on many leaf images for training computer learning models.

Faced with these challenges, computing-based solutions that employ digital image processing and parametric models have been frequently used in leaf analysis. In recent years, improvements promoted by computing systems have pushed agricultural activities to a new level where automation and data analysis have become indispensable. Today, leaf loss estimation is in smartphone apps [6,7], weeds are being analyzed by intelligent machines [8,9], and sensor integration is creating functional IoT ecosystems for smart farms [10]. In this context, classification models [11,12], semantic segmentation [13,14], transformer encoder [15], and pattern recognition [3,16,17] are among the leading

* Corresponding author at: Federal Institute Goiano, Computer Vision Laboratory, Urutaí GO, Brazil.
E-mail addresses: gabriel.vieira@ifgoiano.edu.br (G.S. Vieira), afonso@inf.ufg.br (A.U. Fonseca), naiane@inf.ufg.br (N.M. de Sousa), julio.ferreira@ifgoiano.edu.br (J.C. Ferreira), jufelix16@gmail.com (J.P. Felix), cabacinha@ica.ufmg.br (C.D. Cabacinha), fabrizzio@inf.ufg.br (F. Soares).

https://doi.org/10.1016/j.inpa.2024.03.001
Received 29 July 2022; Received in revised form 13 February 2024; Accepted 1 March 2024
Available online 2 March 2024

research trends in quantifying biotic stress and estimating defoliation caused by insect herbivory. However, image databases for leaf loss analysis and computational models using lightweight processes still need to be continuously prepared and investigated.

In our previous work, we proposed methods for insect predation detection [3], leaf reconstruction [16], and defoliation estimation [17]. The main limitation of previous models was related to the use of computational memory that limited the number of template images. We also noticed that changing the similarity evaluation metric could optimize the image correspondence evaluation step. In the new version of the method, we started using binary images and overlapping areas in the matching stage (Intersection over Union - IoU). In this sense, we reduce memory usage, increase the number of image templates, reduce processing time, and increase assertiveness to levels comparable to deep neural networks.

Furthermore, the identification of plant features can be used to categorize diversity, identify vegetation types, and classify crop families through relevant patterns contained in their leaves. In this sense, anatomical and morphological studies are applied using leaf characteristics to distinguish plant species with high similarity [18], unusual biologic features [19], and their morphometric geometric properties [20]. In addition, foliar analysis at the laboratory level [21] or by machine learning algorithms [12,22,23] can reveal diseases and guide clinical diagnoses and treatment protocols.

In this regard, agricultural systems use the information that can be obtained from leaves to assist in cultivating plants in both small and large crop production and for local or family subsistence. From monitoring to action, the information about leaves can support effective decisions based on a solid foundation for analysis and conclusions. Thus, this knowledge is an essential instrument to assess plant nutrient status [24,25], guide the use of fertilizers and support pest control practices [9,26], estimate the leaf area index [27], measure foliar loss [6,7,28], monitor plant diseases [11,29,30], and identify insufficient nutritional resources in crop management [31].

Among the applications developed from leaf analysis, estimating foliar loss is crucial for planning sustainable agricultural practices. As leaves are inputs for monitoring, evaluation, and decision-making, the analysis process will be impacted if they are compromised, leading to inaccurate results. Therefore, estimating the leaf tissue consumed by insects is a primary practice for conducting inspection methodologies and performing control services in crop fields. Among the defoliation estimation approaches, there are traditional methods that use manual instruments and operator expertise and contemporary approaches that use computer-aided methods and automated models of foliar analysis. Some approaches use visual evaluation and manual quantification [32,33] and predictive models of leaf dimensions [34,35]. In contrast, others include integrative equipment for leaf analysis [36,37], generation of mathematical models using digital image processing techniques [38,39], and deep learning algorithms [7,28,40].

In this study, we employed the template matching technique, which has been traditionally used to solve several problems based on pattern recognition. Template matching has attracted the attention of the computer vision community in recent years [41] and has been successfully applied in biometric and facial recognition [42] as well as in detecting objects in robotics and moving targets [43]. Agriculture also employs template matching to count trees [44], weed detection [45], navigation systems [46], and others. To the best of our knowledge, we are the first to use template matching to construct a method for leaf loss estimation.

In designing our proposal, we considered the limitations of related works to propose a computer-based solution for defoliation estimation. In the proposal, we eliminate aspects of subjective interpretation, deal with many leaf samples in different crop fields, and provide visual indications of the leaf regions where the damage occurred, including border regions. In addition, we can use conventional cameras, build the templates without involving image annotation and training, and acquire the images at different rotation angles, scale variations, and image intensities. The database used in the experimental tests supports these statements since it has different variations, as shown in Fig. 1. Furthermore, the proposed method has lightweight processes that can be executed on time with a final response in a few seconds. In this sense, (1) we present an automated defoliation estimation method whose effectiveness and generalization capacity is evaluated considering different plant species: apple, blueberry, cherry, corn, grape, peach, pepper, potato, raspberry, soybean, strawberry, and tomato; and (2) we organized and made our program code and experimental data publicly available, including an image database that can be used for defoliation estimation purposes.

Our method was developed to assist experts and farmers in monitoring insect predation by analyzing leaf stress caused by defoliation. Severity levels are calculated, and the method's precision in estimating leaf loss can help understand crop health and support agricultural management decisions. In this program version, images can be captured by conventional cameras and processed on a workstation. In future versions, we intend to launch a smartphone application so that processing can be done directly on the device.

The main contributions of this work are:

- a new method that estimates leaf tissue lost both in internal damage and leaf edge regions.
- a comprehensive approach that enables numerical analysis and visual inspections of foliar damage.
- an architecture with well-defined processing steps.
- experimental results with supplementary material to support future comparative analysis (benchmarking).

The remainder of the paper is structured as follows. Section 2 provides key information about the database used and general setup settings (Section 2.1), presents details of the proposed method, its mathematical formulae, and visual descriptions of the workflow (Section 2.2), and also describes the experimental design and evaluation metrics used (Section 2.3). Section 3 presents the test results and a discussion about them. Finally, the work is concluded in Section 4.

2. Material and methods

2.1. Material

The experiments are performed in a public dataset with several specimens of plant leaves: apple, blueberry, cherry, corn, grape, peach, pepper, potato, raspberry, soybean, strawberry, and tomato. We also considered different levels of defoliation severity, with damage to border regions and inner leaf areas. This section presents general information about the conduction of the experiments, the database used, and the selected evaluation metrics.

2.1.1. Image database description

The database used in the experiments was prepared by [47] and it is available online[1] as a result of [48]. It consists of a collection of 54,302 images divided into 14 crops species: Apple (*Malus pumila*), Blueberry (*Vaccinium* spp.), Cherry (*Prunus avium*), Corn (*Zea mays*), Grape (*Vitis vinifera*), Orange (*Citrus sinensis*), Peach (*Prunus persica*), Bell Pepper (*Capsicum annuum*), Potato (*Solanum tuberosum*), Raspberry (*Rubus idaeus*), Soybean (*Glycine max*), Squash (*Cucurbita* spp.), Strawberry (*Fragaria ananassa*), and Tomato (*Solanum lycopersicum*).

Each group has healthy and infected leaves of cultivated plants, labeled by plant pathology specialists (Table 1). In obtaining the samples, technicians collected leaves by removing them from plants and placing them against a sheet of paper that provided a gray or black background

[1] https://github.com/digitalepidemiologylab/plantvillage_deeplearning_paper_dataset

Fig. 1. Samples of soybean leaves in [47] database.

Table 1
Number of images in the database [47].

Crop specie	Healthy leaves	Infected leaves	Total
Apple	1,645	1,526	3,171
Blueberry	1,502	–	1,502
Cherry	854	1,052	1,906
Corn	1,162	2,690	3,852
Grape	423	3,640	4,063
Orange	–	5,507	5,507
Peach	360	2,291	2,651
Pepper	1,478	997	2,475
Potato	152	2,000	2,152
Raspberry	371	–	371
Soybean	5,090	–	5,090
Squash	–	1,835	1,835
Strawberry	456	1,109	1,565
Tomato	1,592	16,570	18,162

to begin acquiring digital images. They sought a variety of lighting conditions, positioning, and foliar shapes. For crops such as Corn and Squash, whose leaves are too large to capture in a single frame, they took images of different sections of the same leaf. The size of the images is 256 × 256 pixels.

The leaves in this database were infected with bacteria, mold, viruses, or mites. Although these pests present foliar deformation, they do not necessarily result in leaf area loss as occurs in situations of herbivory by insects. Because of that, our attention is focused only on images of healthy leaves. We use them to build image models of cultivated species and to prepare artificial defoliation to simulate and assess the losses caused by insect predation. Since Orange and Squash species do not have healthy images in this database, they are not used to evaluate the proposed method. Besides, images of infected leaves from the remaining crop species are not used.

Fig. 1 presents some samples from the database used in this work. Images can be observed under a range of conditions, such as leaves positioned to the right or left (1(a) and 1(b)), in perspective projection 1(c), with shadows 1(d) and in a substantially different format from the others 1(e). Also, changes in illumination can be easily seen in all of these samples, some of them with the *petiole*,[2] (1(a) 1(b) and 1(d)), and others with an incomplete margin — curled leaves 1(e).

2.1.2. General setup

In the proposed method, a damaged leaf is compared to template images, and the result obtained is used to estimate defoliation. First, the dataset is divided into two parts: one equivalent to 80% is used to construct template images, and another with the remaining 20% is used for evaluation purposes. Then, template images are constructed from healthy plant leaves, where a model is prepared for each plant species. The dataset is randomly split. For convenience, we use images that have been previously segmented with the [48] method, which is also available online with the entire dataset (Section 2.1.1). We started the process with image binarization, rotation transformation, and scale adjustment to construct template images and adjust damaged input leaves as presented in Section 2.2.1. Besides, the images selected for evaluation are preliminarily deformed to simulate defoliation as presented in Section 2.3.1. Applying synthetic damage to leaves simulates real cases of herbivory and enables the analysis of different degrees of defoliation severity. Leaf damage is applied in different amounts, which include minor damage ranging from 1 to 15%, medium damage from 16 to 30%, and severe damage from 31 to 45%. Furthermore, the damage is randomly constructed and presented both in the inner leaf area and the leaf edge regions. The image matching process (Section 2.2.2) consists of comparing an injured leaf with all the template images to obtain the most suitable model for leaf analysis. The experiments were done in a notebook with Core i7-9750H (2.6 GHz; 12 MB Cache) and 16 GB RAM. The code was written using MATLAB and is available online.[3]

2.2. Methods

The proposed method is divided into three main steps. In the first one, template images are prepared considering the structural shapes of healthy leaf samples. In the second one, images of damaged leaves are compared with the template images, and the results with the highest similarity are used to locate damaged areas and estimate the percentage of leaf loss (defoliation). Finally, in the third one, defoliation is estimated. We designed the proposed method to support image scale and rotation transformations and to estimate defoliation at different severity levels. The present proposal was also designed to support leaf analysis in different plant species and to delineate damage internally and in leaf edge regions. Fig. 2 shows an overview of the proposed method.

2.2.1. Preprocessing

Initially, RGB images are binarized to differentiate leaf regions (foreground) from non-leaf regions (background). The binarization process is done automatically based on a color threshold that differentiates pixel intensities in the leaf region from other levels of color intensities. Our image database was segmented using the [48] method. Then, the resulting images have black pixels (background) and green color intensities (leaf). Because of that, we apply a simple strategy of labeling each image coordinate with pixels equal to 0 in the three RGB image channels as the image background. In this way, the remaining pixels are set as the target image (foreground).

After binarizing the image, the points in the image foreground are used to compute the smallest convex polygon that contains all the points of the leaf area in a computing process known as “convex hull”. Following that, a morphological operation is applied to the resulting image to trace the leaf silhouette. Each point belonging to the contour of the leaf image is a coordinate in the image plane, which is used

[2] Petiole is a foliar structural component that attaches leaves to the plant stem.

[3] https://github.com/gabrieldgf4/insect_defoliation

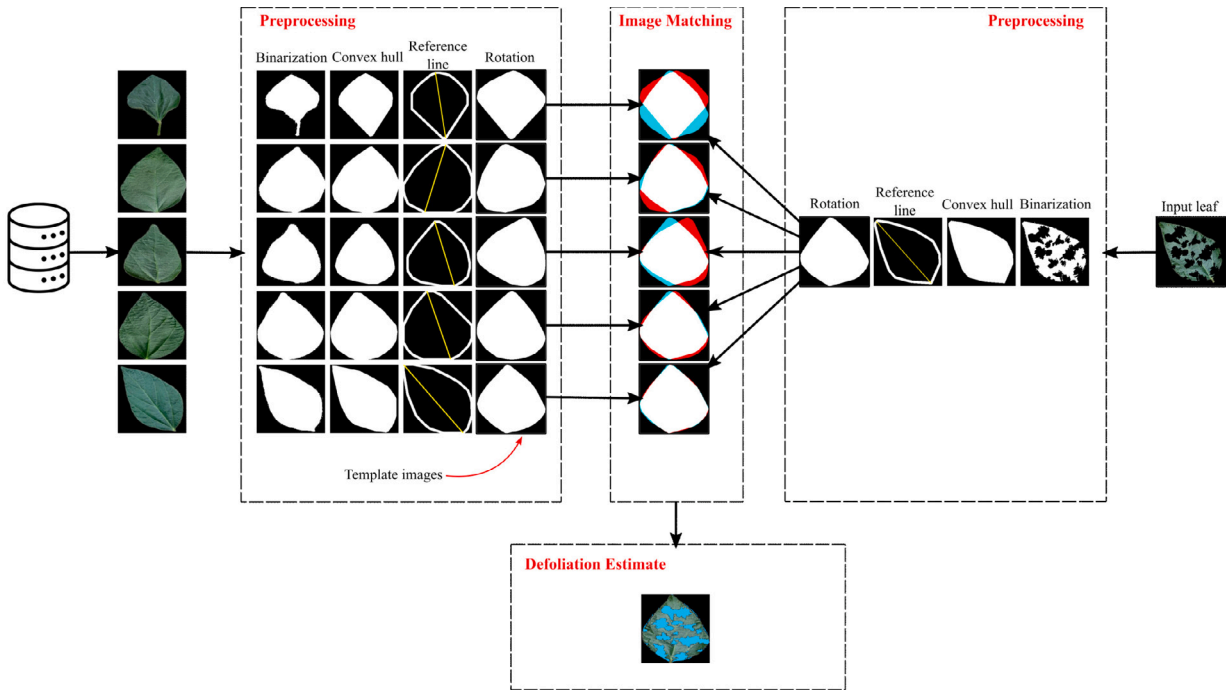

Fig. 2. Overview of the proposed method.

to measure the distance of a given point from the other points. By calculating the distance between all points on the leaf silhouette, we can obtain the two points with the longest distance to represent a pattern that marks an important leaf structure feature, i.e., plants of the same species have similar leaf shapes. Because of this, their width or length can be measured from specific points that are usually in the same positions, even on different leaf samples.

We consider the Euclidean distance between its coordinate pairs to calculate the distance between the leaf silhouette points. From there, a line (reference line) is drawn to connect the two coordinate pairs farthest from each other. The slope angle of this line is computed and used to rotate the image. The rotation operation positions the reference line vertically concerning the abscissa axis by ninety degrees. The leaf area is bounded, cropped, and resized to the original image size in the resulting image. The processes performed at this stage reduce the challenges related to image scale and rotation transformations inherent to image acquisition. As the images are pre-adjusted following the geometric shapes of leaves, it is not necessary to formulate strict protocols for obtaining images nor to prepare images at different angles of inclination for image matching. All these preprocessing steps are applied to constructing template images and adjusting and positioning damaged leaf images.

2.2.2. Image matching

This step establishes a statistical measure to compare a damaged leaf sample with the template images. The objective is to find an image model that best fits the foliar area of the damaged leaf and more effectively highlights the areas of defoliation. In the comparison, we take an exemplar of the template images and compute the points in common between the image template and the damaged leaf. We also compute the total area occupied by the two images being compared. Then, the image similarity is measured by the ratio between their common points (intersection) and their combined areas (union). This process is repeated for all images in the image models, and the comparative result of the highest similarity is used to point out the ideal image model to estimate leaf loss. The image matching process is measured according to Eq. (1), known as IoU [49], Jaccard index [50], or Q_{seg} [51].

$$S = \frac{\sum_{i=1}^{m}\sum_{j=1}^{n} d_{i,j} \wedge t_{i,j}}{\sum_{i=1}^{m}\sum_{j=1}^{n} d_{i,j} \vee t_{i,j}}, \tag{1}$$

where $d_{i,j} \in \mathbf{D}$ is the damaged leaf ($d_{i,j} = 1$) or background pixels ($d_{i,j} = 0$) and $t_{i,j} \in \mathbf{T}$ is the template image, also in a binary format. The accuracy is based on logical operations, logical *and* ($\wedge$) and logical *or* ($\vee$), that compare the overlap between the template image **T** and the damaged leaf **D**. S varies in a range of values between 0.00 and 1.00 in which a value of 1.00 represents a perfect consistency outcome between **D** and **T** images. **D** and **T** are binary images with size m by n.

2.2.3. Defoliation estimate

The defoliation estimate is calculated from the logical conjunction between the selected template image and the damaged leaf. As these images are in binary format, the leaf area of the template image that is outside the scope of the damaged leaf delineates its loss regions. It is important to note that plant leaves from the same crop field have very similar characteristics, so matching between image pairs and image area overlap calculation can enable consistent results in defoliation estimation. Thus, the task consists of counting the points outside the intersection between the image pairs. In Eq. (2), we have two binary images (**T** and **D**) corresponding to the damaged leaf and retrieved template image, respectively. The logical conjunction ($\wedge$) between them results in image **L**, which is the estimated missing area from image **D**. The image **L** is constructed by fetching the regions of **T** that are not in **D**. Thus, the symbol ($\neg$) refers to the complement of **D**.

$$\mathbf{L} = \mathbf{T} \wedge \neg\mathbf{D} \tag{2}$$

After that, the percentage of pixels in **L** is calculated according to Eq. (3),

$$p(\%) = \frac{100}{mn}\sum_{i=1}^{m}\sum_{j=1}^{n} l_{i,j} \tag{3}$$

where $l_{i,j} \in \mathbf{L}$ and m and n denote the number of rows and columns in the image **L**, respectively. p is the percentage of the defoliation level.

2.3. Experimental design

2.3.1. Synthetic defoliation strategy

Considering that a visual diagnosis is possible by a human, computational tools, in principle, can also assist in this task. The challenge is to

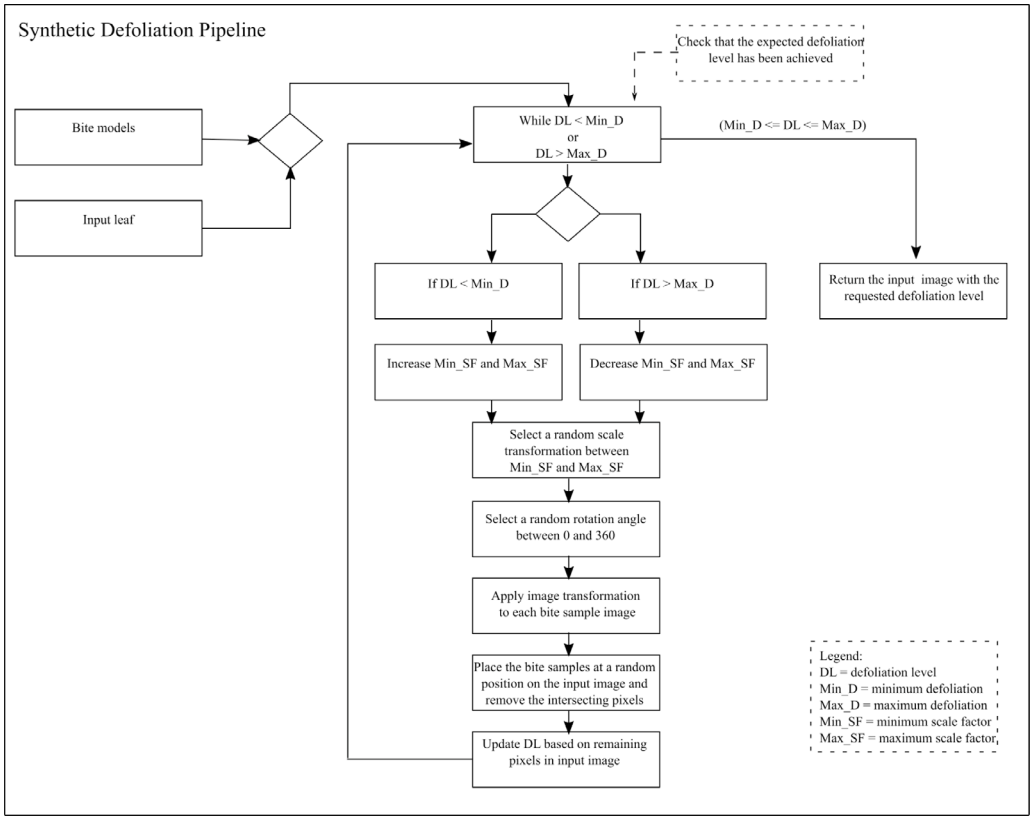

Fig. 3. Pipeline for applying damage to leaf images.

find sufficiently expressive samples to allow inferences from computer vision models, which is even more complicated when data labeling requires specialized manual labor, which can be time-consuming and expensive. To overcome this problem, we have prepared a synthetic defoliation strategy in which healthy leaves are subjected to a process capable of simulating leaf area loss.

Our insect predation strategy on leaves involves extracting bite signatures in real herbivory cases and preparing foliar damage templates to promote different leaf defoliation levels. The bite signature of two types of insects, *Spodoptera Frugiperda* and *Chrysodeixis Includens*, was extracted from injured leaves, resulting in some bite samples for each of the two insects.

Considering previously collected bite samples, we built a program that uses the bite samples to generate leaf damage automatically. This program simulates insect predation considering the number of bite samples and the minimum (Min_D) and maximum (Max_D) expected defoliation level (which can range from 1 to 99%). Fig. 3 illustrates the pipeline used in our synthetic defoliation strategy, where an input image is processed with the bite samples. The program applies image transformations (scale and rotation) to the bite samples and uses them to remove pixels from the input image. The scale factors (Min_SF and Max_SF) are dynamically adjusted, and the rotation angle is randomly set in the range 0 to 360. The program iteratively manipulates these two variables until the desired defoliation level is reached. In the program, DL is initially set to 0, which is updated with changes made to the input leaf image. When the expected defoliation level (DL) is achieved, the input image with the requested defoliation level is returned. Additionally, Fig. 4 shows the process of applying leaf damage to an input leaf, while Fig. 5 presents some defoliation results generated by the program. This strategy is used to obtain the reference values (ground-truth data) in the experimental tests in Section 3.

2.3.2. Evaluation metrics

To quantify the results, we used statistical measures to analyze the reliability of the statistical relationships. The problem was modeled as a binary classification test in which the samples were labeled as damaged leaf area or non-damage leaf area. The rating assigned as correct or incorrect is measured according to the number of pixels counted and is defined as:

- True Positive (TP): damaged leaf area correctly identified as damaged regions;
- True Negative (TN): non-damaged leaf area correctly identified as non-damaged regions;
- False Positive (FP): regions categorized as damaged areas when they are not.
- False Negative (FN): damaged regions that have not been properly recognized.

In the analysis of the results, we used the statistical measures TPR (true positive rate, Eq. (4)) and TNR (true negative rate, Eq. (5)) to indicate the fraction of areas of leaf damage that were successfully recovered. Likewise, we consider the FPR (false positive rate, Eq. (6)) and FNR (false negative rate, Eq. (7)) to measure the percentage of incorrectly classified defoliation areas. TPR, TNR, FPR, and FNR are used in the construction of confusion matrices to show the performance of our method in the different types of plant species investigated in this study.

$$TPR = \frac{TP}{TP + FN} \tag{4}$$

$$TNR = \frac{TN}{TN + FP} \tag{5}$$

$$FPR = \frac{FP}{FP + TN} \tag{6}$$

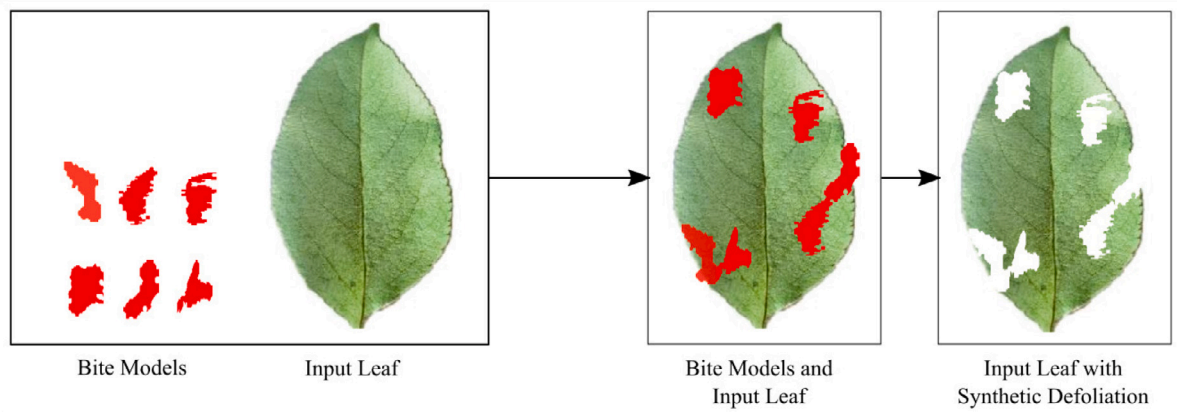

Fig. 4. Synthetic defoliation strategy.

(a) Original. (b) 11.67% defoliation. (c) 27.69% defoliation. (d) 53.97% defoliation.

Fig. 5. Samples from the synthetic defoliation strategy after segmentation.

$$FNR = \frac{FN}{FN + TP} \tag{7}$$

Jaccard (Eq. (8)), *Dice* (Eq. (9)), and *accuracy* (ACC, Eq. (10)) indices are also used to provide single measures related to the percentage of the identified defoliation regions. All metrics presented range from 0.00 to 1.00, in which higher results of TPR, TNR, *Jaccard*, *Dice*, and *accuracy* point to better assertiveness. On the other hand, values of FPR and FNR close to zero indicate fewer errors in the interpretation and determination of damaged leaf areas.

$$Jaccard = \frac{TP}{TP + FP + FN} \tag{8}$$

$$Dice = \frac{2 \cdot TP}{2 \cdot TP + FP + FN} \tag{9}$$

$$ACC = \frac{TP + TN}{TP + TN + FP + FN} \tag{10}$$

Besides, the linear correlation between the expected and estimated defoliation level is measured with Pearson's correlation coefficient (r), which indicates the degree of relationship between two quantitative variables and expresses the degree of correlation through values between −1 and 1 [52]. The correlation is calculated according to Eq. (11) as follows.

$$r = \frac{\sum_{i=1}^{n}(x_i - \bar{x})(y_i - \bar{y})}{\sqrt{\sum_{i=1}^{n}(x_i - \bar{x})^2}\sqrt{\sum_{i=1}^{n}(y_i - \bar{y})^2}}, \tag{11}$$

where x contains the reference leaf damage values obtained from the synthetic defoliation strategy, and $\bar{x}$ is the average value of these defoliation levels. y contains the estimated leaf damage values, and $\bar{y}$ is the average value of the estimated defoliation levels. n represents the number of images in the dataset for a plant species being evaluated.

Moreover, according to Eq. (12), Root Mean Square Error (RMSE) computes the error between the reference leaf damage (x) and the estimated leaf damage (y).

$$RMSE = \sqrt{\frac{\sum_{i=1}^{n}(x_i - y_i)^2}{n}} \tag{12}$$

3. Results and discussion

In this section, the results obtained with the experimental tests are presented. The effectiveness of the proposed method is verified in different plant species, and the results are discussed considering three main points: correctness in the identification of missing segments of leaf area, assertiveness in the defoliation estimation, and precision in the visual representation of the damaged leaf with its defoliation regions. We also present a qualitative comparison between our method and some related works, discuss the limitations of the proposed method, and present information about the execution time. To obtain the reference data (ground truth), we used the strategy presented in Section 2.3.1.

3.1. Damaged area identification

Damaged areas, or areas of defoliation, are leaf regions that have been consumed and are no longer present in the image. Identifying these areas consists of predicting the regions that suffered losses and locating them. Thus, it is possible to visually show the leaf canopy, including the regions that suffered defoliation. The evaluation consists of verifying the overlap of the estimated areas with the actual losses to point out the precision in identifying the damaged areas. In this regard, the *Jaccard* and *Dice* indices were used to measure the level of overlap and confusion matrices to measure the percentage of correctly categorized pixels.

Table 2 presents the results for defoliation levels between 1 and 15%, 16 and 30%, and 31 and 45%. As can be seen, the indicators show very little difference between the results, and the size of the leaf damage has little influence on the final results. In most cases,

Table 2
Statistical measures of identifying damaged leaf area in different defoliation levels.

	Defoliation: 1–15%			Defoliation: 16–30%			Defoliation: 31–45%		
	Jaccard	Dice	ACC	Jaccard	Dice	ACC	Jaccard	Dice	ACC
Apple	34.9	49.8	94.8	57.3	72.2	93.1	63.7	77.3	90.0
Blueberry	34.6	49.7	94.6	59.1	73.9	92.2	66.1	79.3	90.9
Cherry	36.6	51.3	95.8	61.1	75.3	94.2	65.5	78.6	91.8
Corn	85.0	91.6	99.6	82.8	89.9	98.2	82.2	89.1	96.7
Grape	33.6	49.0	94.6	59.7	74.6	93.1	66.0	79.3	90.0
Peach	20.1	31.6	91.0	45.0	61.0	89.5	51.5	67.0	87.2
Pepper	33.8	48.6	95.0	58.7	73.5	93.5	65.1	78.4	91.5
Potato	37.0	52.7	95.2	60.7	75.2	93.4	67.3	80.2	91.7
Raspberry	38.5	53.8	95.7	62.1	76.2	94.3	69.9	81.5	92.6
Soybean	47.3	62.5	97.1	68.5	81.0	95.5	71.6	83.0	93.2
Strawberry	36.3	51.7	95.5	63.4	77.4	93.8	69.4	81.7	91.8
Tomato	31.5	45.7	94.0	54.3	69.8	92.5	61.7	75.8	90.5

the accuracy (ACC) was more significant than 90%. However, it is noted that higher levels of defoliation slightly degrade the accuracy. As damage severity increases, leaf edge regions can be compromised, altering leaf structure and leading to erroneous estimates. Therefore, the results are more accurate when slight changes in the leaf edges occur. On the other hand, the values of $Jaccard$ and $Dice$ increased with more damage to the leaves. When the damage is minor, the injured leaf adjusts less to the template images, leaving artifacts near the leaf edges that do not overlap with the actual damage.

Fig. 6 presents confusion matrices with percentages of correct answers (TPR and TNR) and errors (FPR and FNR) for the plants under study. The data for calculating these matrices were obtained with defoliation levels from 1 to 45%

3.2. Defoliation estimate

The level of defoliation is measured by the linear correlation between the actual and the estimated loss. When there is a strong correlation, the error effect is considered minimal, although randomly distributed around the regression line. Fig. 7 shows scatter plots for the different types of crops investigated in this study. Blueberry, Corn, Grape, Potato, Raspberry, Soybean, and Strawberry obtained a correlation coefficient greater than 0.96 where Blueberry and Raspberry reached $r = 0.97$, and Grape, Potato, Soybean, and Strawberry reached $r = 0.98$, and Corn reached $r = 0.99$. Apple, Peach, and Tomato obtained lower results than the others, with values equal to $r = 0.93$, $r = 0.77$, and $r = 0.92$, respectively. Corn obtained the most accurate result due to the leaf region occupying the full image size. On the other hand, Peach and Tomato obtained less accurate results mainly due to the irregular pattern caused by the intensity of shading on peach leaves and the registration of different tomato species with early and adult leaves. Despite this, the results show that the method can be generalized for different plant species and is consistent at different levels of leaf damage.

However, it is important to note that the estimation error differs somewhat according to the plant species. Leaf structures have their own characteristics that identify them and differ from other types of crops. For plants with more homogeneous characteristics, such as soybeans, leaf models can better represent the set. When the specimens have variations in shape caused by the stage of leaf maturity, type of cultivar, or shading in leaf regions, as in tomato, apple, and peach, the leaf models may be less assertive. In this way, the results are linked to the conditions of the image database. Also, for this reason, the estimated error can differ from the actual error. Our method often overestimates the error estimate, indicating that the leaf models have a larger leaf area than the test set images. For leaf analysis situations, these results could better alert for preventive decision-making actions than underestimated results that could erroneously postpone safeguarding actions.

3.3. Visual inspection

In addition to estimating the percentage of defoliation, in our proposal, the damaged leaf regions are visually presented. It is a handy feature because it allows the analyst to check which points in the leaf region are being attacked. For example, some chewing insects initiate defoliation from the inner vein to the edges of the leaves. In contrast, cutting insects prefers to start from border regions. Therefore, visual information like the one we present can support other analyses besides the leaf loss estimate. Fig. 8 shows some cases of defoliation and presents percentages of leaf tissue consumed and estimated for different levels of leaf loss.

Some detection error is justified by the number of spurious pixels resulting from the image binarization process, leading to differences between the leaf template and the test leaf. The binarization step may associate points in the leaf edge region with the area of interest when, in fact, they should be categorized as the background region. This effect can be visually observed in Fig. 8, especially in the images of grape and strawberry leaves ((e) and (k)). Besides that, the image template may not correctly fit the shape of the test image, leading to differences between the two images. As the preprocessing stage applies image adjustments through rotation transformation, the template, and test images can be in different profiles, making it difficult to match them. In addition, the level of defoliation severity can influence the image's positioning, as seen in the corn leaf (Fig. 8 (d)). In this case, the three images originated from the same test leaf, but due to the level of defoliation, they were rotated and placed in different positions. Also, it is worth mentioning that the actual damaged percentage is obtained with the synthetic defoliation strategy (Section 2.3.1), in which the defoliation level is computed based on the damages applied to input images.

3.4. Comparative analysis

A direct comparison between related works is quite challenging as no benchmarking exists. Because of this, researchers use their database, which is not accessible to the general public. Then, the data are restricted to those presented in the published works, and it is hard to verify the samples' variability, such as lighting conditions, leaf format and position, and background complexity. Also, leaf images with damage caused by real insects or artificial leaf canopy damage used in experimental tests are difficult to reproduce to compare the results. Despite this, we present a comparative analysis between our method and related works considering only soybean leaves. Fig. 9 shows that the linear correlation (r) obtained by our method is better than using a digital scanner [53] and as assertive as Bioleaf [6], which is a semi-automatic method, and AlexNet, a convolutional neural network. Also, Fig. 10 shows that the RMSE score of our method is smaller than those presented by the deep neural networks AlexNet, VGGNet, and ResNet [28].

Fig. 6. Confusion matrices for different plant species.

Additionally, we qualitatively compare our work with related work. Unlike [29,54], the estimates performed in our proposal are fully automated so that computer-assisted processes obtain the results. Likewise, our work differs from [6] because our method does not require user interaction and operator expertise to define leaf edge contours. It differs from [28,40] since our proposal does not use training steps, which are time-consuming and require many images to converge the models. It also differs from [7] because our model can estimate the severity of leaf stress caused by chewing and cutting insects. Furthermore, our proposal does not require specific equipment such as those used in manual quantification or leaf area measurement equipment [55,56]. Also, we demonstrate the generalization of our proposed method by considering different types of plant species. Finally, our experimentation differs substantially from the other works as we use a public database that is available online and many validation metrics, including visual inspections.

In this sense, to address the problem related to the complexity of quantitative comparisons, we organized our experimental data and made them available as supplementary material.[4] We indicate the images used in the construction of template images and those used in the tests. For the test images, we indicate their defoliation percentage in three groups: from 1 to 15%, 16 to 30%, and 31 to 45%. Fig. 11 presents some examples used in the performance evaluation, which are available in the supplementary material.

3.5. Time performance analysis

The time to execute the leaf analysis processes depends on the number of images used to construct the template images. Therefore, processing will require more time for a more significant quantity of template images. Table 3 shows the average execution time and standard deviation of the three processing steps considering the number of images used in the template image construction and the number

[4] https://github.com/gabrieldgf4/insect-defoliation-dataset

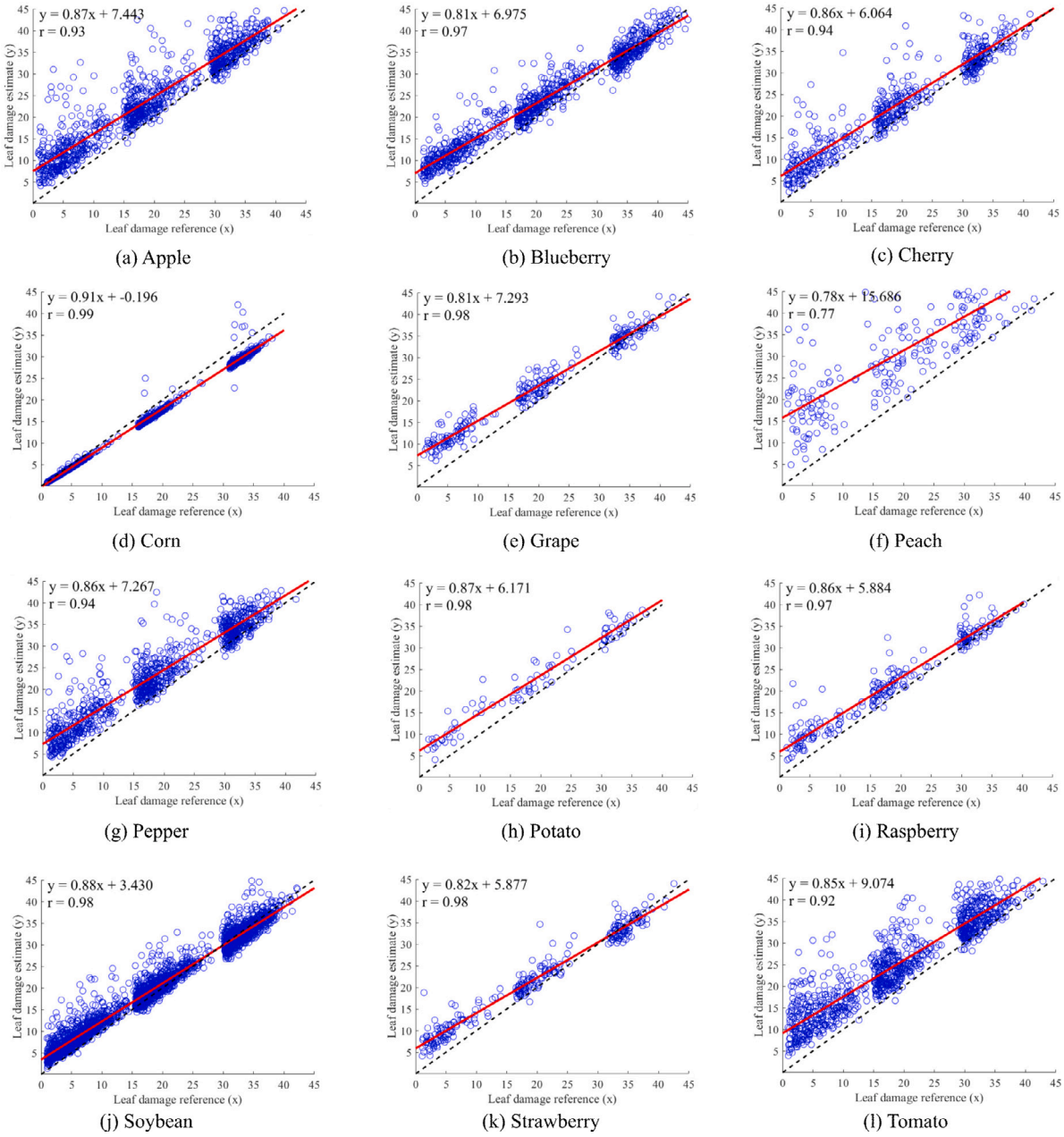

Fig. 7. Linear correlation of the proposed method in 12 different crop species.

of images used as test images. The most time-consuming task is related to image preprocessing. In this task, we need to binarize the image, compute its convex hull, find a reference line, and perform image rotation. The last two operations are the most time-consuming. However, each presented time in Table 3 represents the total time for each plant sample group. We highlight that the preprocessing time for a single image sample is about three milliseconds, which can be considered small. In any event, we believe that is not significant since modern approaches with parallel computing can significantly reduce the preprocessing time.

It is worth mentioning that the preparation of the template image is performed only once, so the final result can be quickly obtained. Also, the number of images used to construct the template and test images varies according to the plant species in the dataset. As we evaluate our proposal at three defoliation intervals, the number of test images is multiplied by three.

3.6. Limitations

Although the proposed method presents consistent results, mentioning some of its limitations is essential. First, results are more assertive when the leaf samples have a regular pattern in their shape. In this way, image templates can better represent groups of plant species and find better matches for damaged leaves. Furthermore, the segmentation process that separates the leaf canopy (foreground) from the rest of the image (background) can influence the results since the image templates may contain areas outside the leaf region. Therefore, complex backgrounds and multiple plant leaf samples per image can deteriorate the method's performance.

Problems related to background permeate all leaf analysis proposals. Related work deals with this problem by suggesting using a blank sheet of paper to differentiate the target object from the background or simply using databases with the target object already segmented.

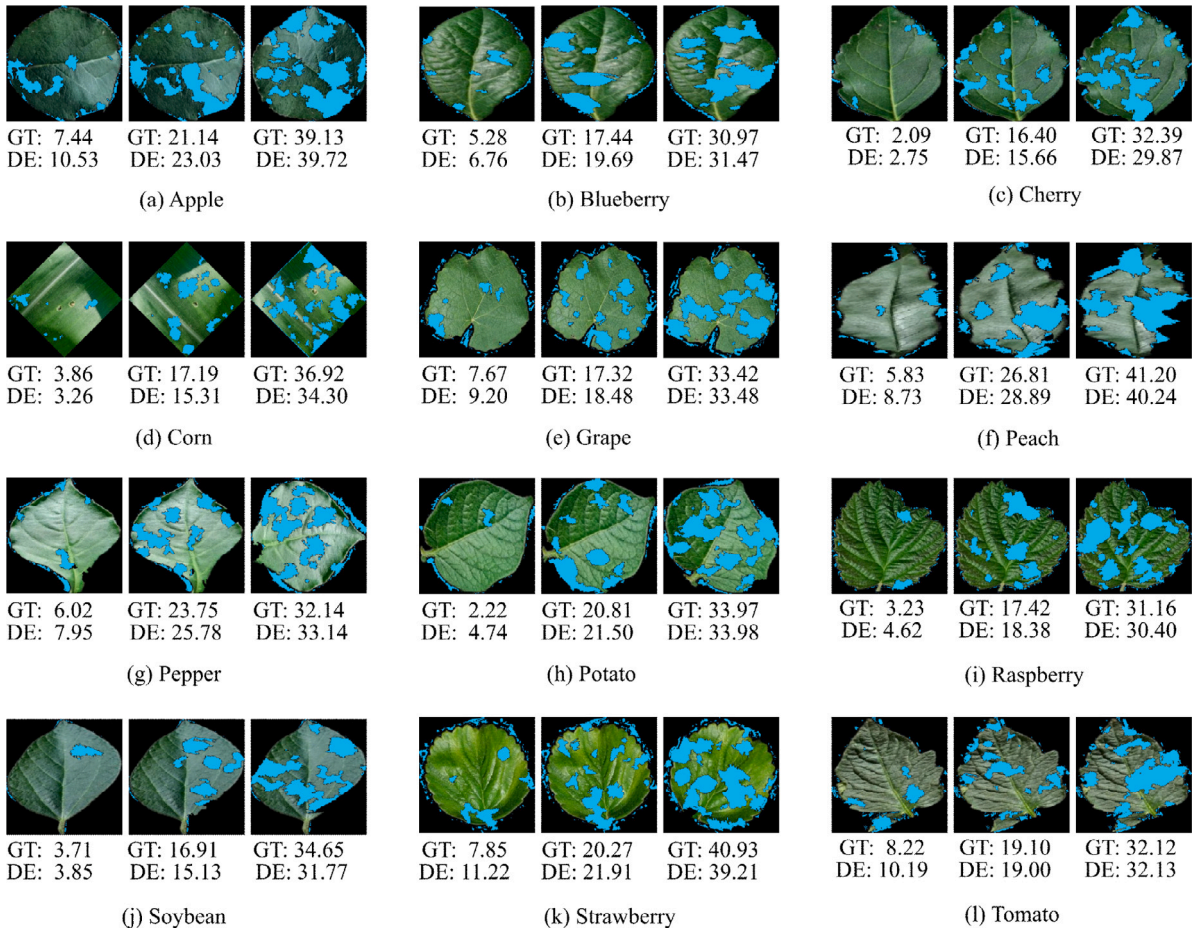

Fig. 8. Estimated defoliation areas (in blue) and percentage of actual leaf damage and leaf damage estimated by the proposed method. (GT = ground truth, DE = defoliation estimate).

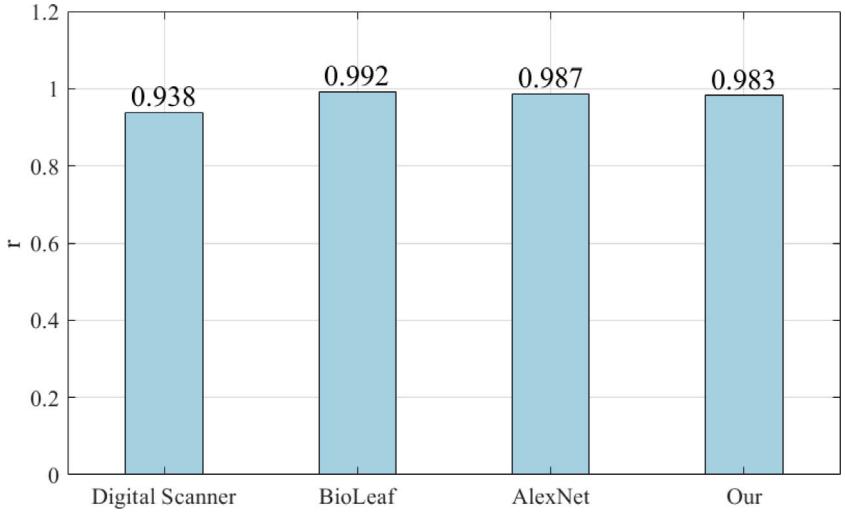

Fig. 9. Comparative considering linear correlation (r).

Background subtraction and semantic segmentation are typical computer vision problems and expand the scope of our investigation. These are topics of interest for future work, where we intend to investigate segmentation methods and apply them in scenarios with a complex background. Therefore, we plan to add new pre-processing steps in future versions of the proposed method to deal with two or more leaves in the same image and multiple overlapping leaves.

We have included a comprehensive figure to present some simulations concerning complex conditions. Fig. 12 presents a test leaf whose background was not removed, another sample with a bigger and a smaller leaf in the same image, a shaded image, and a leaf image with the stalk (petiole) that attaches the leaf blade to the stem in a severe defoliation condition. In all cases, the estimated error differs from the actual error because none of the image templates fit the test leaves

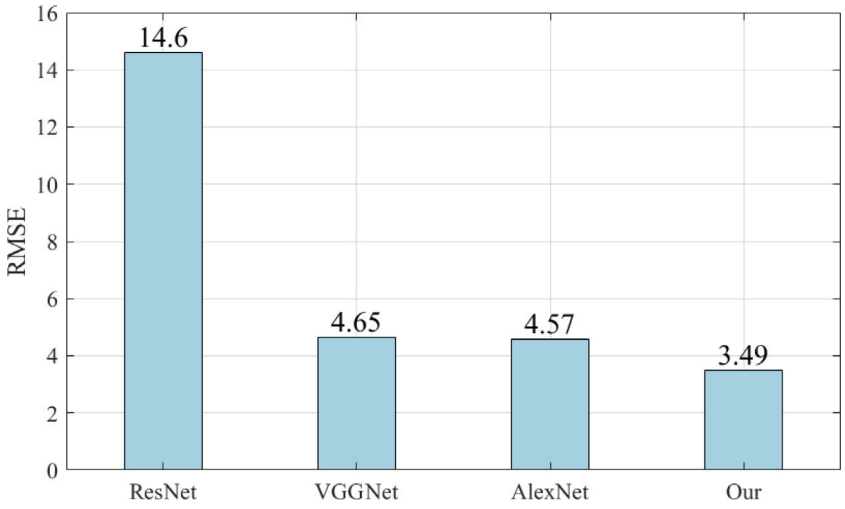

Fig. 10. Comparative considering RMSE.

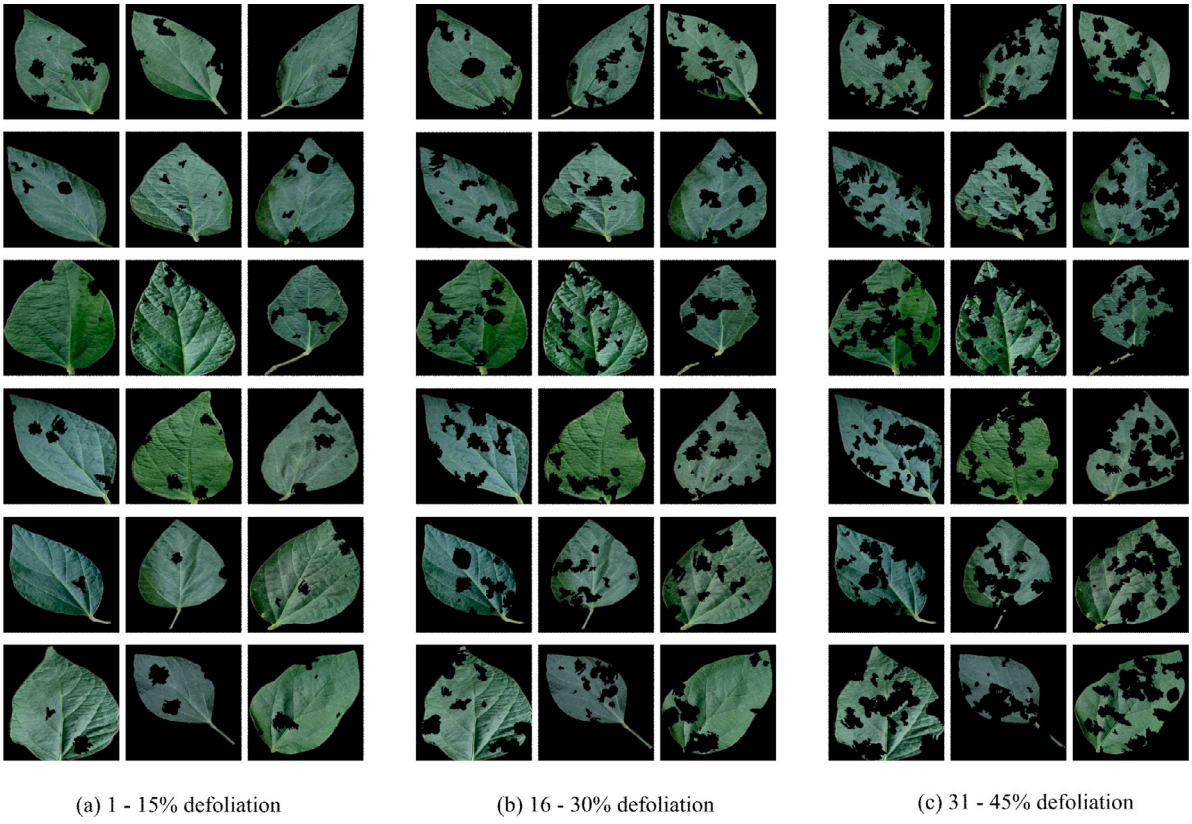

Fig. 11. Some samples of the soybean test images.

correctly. Thus, due to the complexity of the scene as a background region associated with the region of interest, more than one leaf per image, image shadows that limit binarization, test leaf shapes that differ from leaf templates, and excessive leaf damage, the method's accuracy may deteriorate.

However, these issues can be overcome with more homogeneous databases and image acquisition with attention to background simplification. In practice, leaf analysis is performed on homogeneous crop types, and leaf samples are separated according to their position on the plants (e.g., at the top or upper third of the plant). Besides that, image acquisition can be made using a blank sheet of paper as proposed by [6], making it possible to collect data with leaf isolation and without removing the sample for analysis (i.e., a non-destructive approach).

Despite this, through an automatic approach to leaf analysis, the proposal deals with some challenges in estimating defoliation. In this regard, the severity of leaf damage at different levels, the impairment of the leaf surface in edge regions, the difficulty in building generalist models that work in different plant species, and processing steps that are performed in reasonable processing time are addressed in this work to consolidate a tool for precision agriculture. On the other hand, issues related to the collection of leaf samples are not directly discussed in this study. Our work considers a more straightforward color-based segmentation to differentiate regions of interest from background images. Thus, in cases where unfavorable conditions are involved, such as a complex background and more than one leaf per image, other segmentation strategies should be investigated.

Table 3
Execution time (in seconds) of the proposed method steps and the number of template and test images.

	Preprocessing	Image matching	Defoliation estimate	Template images	Test images
Apple	4.22 ± 2.42	0.18 ± 0.01	5.63e−04 ± 3.08e−04	1,316	329 × 3
Blueberry	4.46 ± 2.55	0.18 ± 0.01	4.94e−04 ± 2.52e−04	1,202	300 × 3
Cherry	2.76 ± 1.65	0.14 ± 0.01	5.31e−04 ± 3.23e−04	684	170 × 3
Corn	5.33 ± 3.04	0.15 ± 0.01	5.84e−04 ± 3.48e−04	930	232 × 3
Grape	1.31 ± 0.72	0.12 ± 0.03	6.09e−04 ± 3.63e−04	339	84 × 3
Peach	0.96 ± 0.50	0.11 ± 0.01	6.40e−04 ± 5.63e−04	288	72 × 3
Pepper	4.14 ± 2.40	0.17 ± 0.02	5.27e−04 ± 3.99e−04	1,183	295 × 3
Potato	0.60 ± 0.30	0.11 ± 0.01	5.03e−04 ± 3.26e−04	122	30 × 3
Raspberry	1.15 ± 0.62	0.11 ± 0.01	4.91e−04 ± 2.53e−04	297	74 × 3
Soybean	13.71 ± 7.92	0.37 ± 0.01	4.84e−04 ± 3.01e−04	4,072	1.018 × 3
Strawberry	1.36 ± 0.76	0.11 ± 0.01	5.05e−04 ± 2.83e−04	365	91 × 3
Tomato	4.09 ± 2.38	0.17 ± 0.01	5.42e−04 ± 2.85e−04	1,273	318 × 3

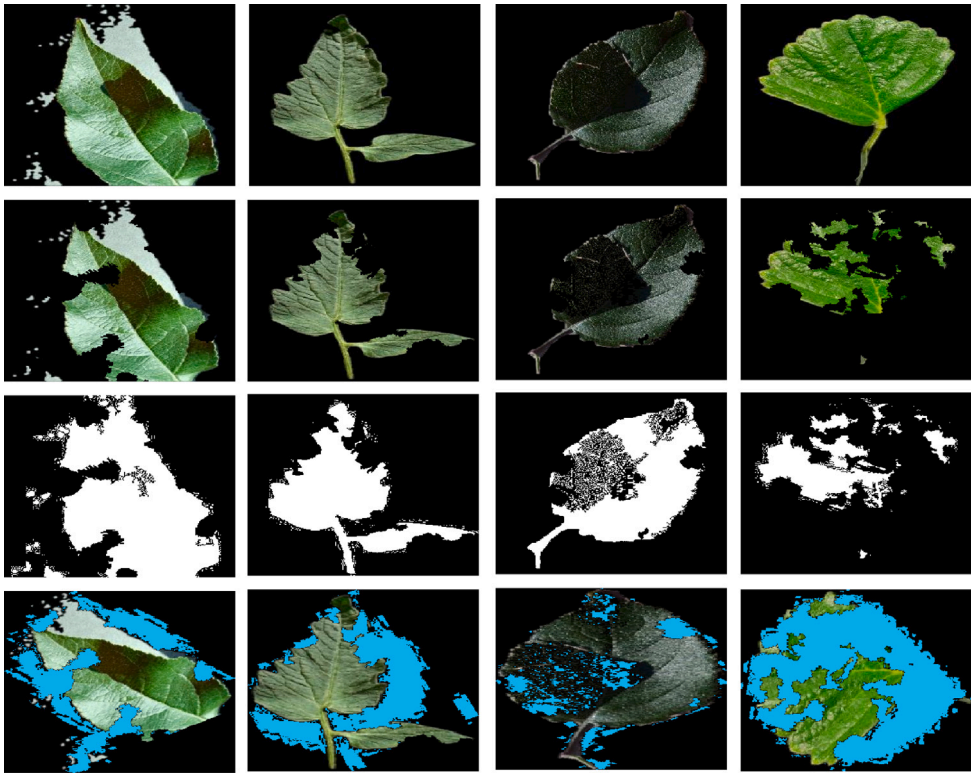

Fig. 12. Limitation of the method. From (a) to (d): inaccurate background removal, more than one leaf per image, shaded leaf, peculiar leaf shape with severe damage. From the first row to the fourth: input leaf, damaged leaf with synthetic defoliation, binarized damaged leaf, defoliation estimated. (GT = ground truth, DE = defoliation estimate).

In a scenario of potential use of our method, an operator captures images with an RGB camera with only one leaf per record. This step could be done with some contrasting background that simplifies the target object segmentation process. An image data set is prepared to contain only healthy leaves, i.e., images with no incidence of insect predation. Likewise, injured leaves are captured and stored in another data set. Then, the method builds template images with the data set of healthy leaves and compares the injured leaves with the templates. Finally, the method returns the estimated percentage of defoliation. In this fashion, the operator does not need to worry about the position of the leaf surface, the distance between the camera and the target image, or the outline of the leaf silhouette. The method was designed to minimize image acquisition effects such as rotation and scale transformations and work without requiring manual delineation of leaf boundary regions. In this study, we use the segmentation method proposed by [48], whose operation is outside the method pipeline. Other segmentation strategies can be investigated to separate the leaf from the image background.

4. Conclusion

In this work, we present a method for estimating leaf damage. As removing leaf tissue from insects reduces photosynthetic capacity, measuring the percentage of leaf area consumed is vital to verify the degree of interaction between insects and crop fields. In this sense, leaf analysis enhances decision-making, contributing to more efficient agricultural management actions and strategies.

The proposed method is suitable for monitoring activities with much greater sampling capacity than in manual or semi-automatic leaf analysis processes. Furthermore, our method can be applied to plant species with various leaf shapes. Likewise, it can accurately estimate defoliation at various severity levels and visually present the area of leaf tissue consumed for further analysis and inspection. Thus, as it has a well-defined pipeline with lightweight processing steps, the proposed method is suitable for devices with limited computational power. Although we can see powerful neural networks, the computational resources to run models and memory to accommodate the size of the weights of these networks are still somewhat limiting. Current trends are easing limitations on computing power, and we will soon see new scenarios. In any case, our method will remain competitive as it can be parallelized to process even larger amounts of data per second.

CRediT authorship contribution statement

Gabriel S. Vieira: Conceptualization, Methodology, Software, Writing – original draft. **Afonso U. Fonseca:** Methodology, Validation. **Naiane Maria de Sousa:** Visualization, Investigation. **Julio C. Ferreira:** Data curation. **Juliana Paula Felix:** Writing – review & editing. **Christian Dias Cabacinha:** Formal analysis. **Fabrizzio Soares:** Writing – review & editing, Supervision.

Declaration of competing interest

We declare that the manuscript “An automatic method for estimating insect defoliation with visual highlights of consumed leaf tissue regions” is original and it is not being considered by any other publishing elsewhere. We have no conflicts of interest to disclose.

Acknowledgments

The authors would like to thank the Universidade Federal de Goiás (Brazil), Instituto Federal Goiano (Brazil), and CAPES (Coordenação de Aperfeiçoamento de Pessoal de Nível Superior – Brazil) [66666622+ CAPES Finance Code #001] for partially supporting this research work.

References

[1] Moraes Rocha B, Ueslei da Fonseca A, Pedrini H, Soares F. Automatic detection and evaluation of sugarcane planting rows in aerial images. Inf Process Agric 2023;10(3):400–15. http://dx.doi.org/10.1016/j.inpa.2022.04.003, URL https://www.sciencedirect.com/science/article/pii/S2214317322000439.

[2] da Silva Vieira G, Rocha BM, Soares F, Lima JC, Pedrini H, Costa R, et al. Extending the aerial image analysis from the detection of tree crowns. In: 2019 IEEE 31st international conference on tools with artificial intelligence. IEEE; 2019, p. 1681–5. http://dx.doi.org/10.1109/ICTAI.2019.00247.

[3] da Silva Vieira G, Rocha BM, Fonseca AU, de Sousa NM, Ferreira JC, Cabacinha CD, et al. Automatic detection of insect predation through the segmentation of damaged leaves. Smart Agric Technol 2022;2:100056. http://dx.doi.org/10.1016/j.atech.2022.100056.

[4] Nabity PD, Zavala JA, DeLucia EH. Indirect suppression of photosynthesis on individual leaves by arthropod herbivory. Ann Botany 2009;103(4):655–63.

[5] Fernandes ET, Ávila CJ, da Silva IF. Effects of different levels of artificial defoliation on the vegetative and reproductive stages of soybean. EntomoBrasilis 2022;15:e991.

[6] Machado BB, Orue JP, Arruda MS, Santos CV, Sarath DS, Goncalves WN, et al. BioLeaf: A professional mobile application to measure foliar damage caused by insect herbivory. Comput Electron Agric 2016;129:44–55.

[7] Esgario JG, de Castro PB, Tassis LM, Krohling RA. An app to assist farmers in the identification of diseases and pests of coffee leaves using deep learning. Inf Process Agric 2022;9(1):38–47. http://dx.doi.org/10.1016/j.inpa.2021.01.004, URL https://www.sciencedirect.com/science/article/pii/S2214317321000044.

[8] Sodjinou SG, Mohammadi V, Sanda Mahama AT, Gouton P. A deep semantic segmentation-based algorithm to segment crops and weeds in agronomic color images. Inf Process Agric 2022;9(3):355–64. http://dx.doi.org/10.1016/j.inpa.2021.08.003, URL https://www.sciencedirect.com/science/article/pii/S2214317321000731.

[9] Luo T, Zhao J, Gu Y, Zhang S, Qiao X, Tian W, Han Y. Classification of weed seeds based on visual images and deep learning. Inf Process Agric 2023;10(1):40–51. http://dx.doi.org/10.1016/j.inpa.2021.10.002, URL https://www.sciencedirect.com/science/article/pii/S2214317321000809.

[10] Andrianto H, Faizal A, Kurniawan NB, Aji DPP, et al. Performance evaluation of IoT-based service system for monitoring nutritional deficiencies in plants. Inf Process Agric 2021. http://dx.doi.org/10.1016/j.inpa.2021.10.001.

[11] Ngugi LC, Abdelwahab M, Abo-Zahhad M. A new approach to learning and recognizing leaf diseases from individual lesions using convolutional neural networks. Inf Process Agric 2023;10(1):11–27. http://dx.doi.org/10.1016/j.inpa.2021.10.004, URL https://www.sciencedirect.com/science/article/pii/S2214317321000822.

[12] Shah D, Trivedi V, Sheth V, Shah A, Chauhan U. Rests: Residual deep interpretable architecture for plant disease detection. Inf Process Agric 2022;9(2):212–23. http://dx.doi.org/10.1016/j.inpa.2021.06.001, URL https://www.sciencedirect.com/science/article/pii/S2214317321000482.

[13] Luo Z, Yang W, Yuan Y, Gou R, Li X. Semantic segmentation of agricultural images: A survey. Inf Process Agric 2023. http://dx.doi.org/10.1016/j.inpa.2023.02.001, URL https://www.sciencedirect.com/science/article/pii/S2214317323000112.

[14] Kolhar S, Jagtap J. Plant trait estimation and classification studies in plant phenotyping using machine vision – a review. Inf Process Agric 2023;10(1):114–35. http://dx.doi.org/10.1016/j.inpa.2021.02.006, URL https://www.sciencedirect.com/science/article/pii/S2214317321000238.

[15] Fu X, Ma Q, Yang F, Zhang C, Zhao X, Chang F, et al. Crop pest image recognition based on the improved ViT method. Inf Process Agric 2023. http://dx.doi.org/10.1016/j.inpa.2023.02.007, URL https://www.sciencedirect.com/science/article/pii/S2214317323000173.

[16] Vieira GDS, de Sousa NM, Rocha B, Fonseca AU, Soares F. A method for the detection and reconstruction of foliar damage caused by predatory insects. In: 2021 IEEE 45th annual computers, software, and applications conference. IEEE; 2021, p. 1502–7. http://dx.doi.org/10.1109/COMPSAC51774.2021.00223.

[17] Vieira GS, Fonseca AU, Rocha BM, Sousa NM, Ferreira JC, Felix JP, et al. Insect predation estimate using binary leaf models and image-matching shapes. Agronomy 2022;12(11):2769. http://dx.doi.org/10.3390/agronomy12112769.

[18] Chimezie E, Ogazie C, Stephen M. Importance of leaf, stem and flower stalk anatomical characters in the identification of emilia cass. Int J Plant Soil Sci 2016;12:1–12. http://dx.doi.org/10.9734/IJPSS/2016/28420.

[19] Silva Ad, Alves MVdS, Coan AI. Importance of anatomical leaf features for characterization of three species of mapania (mapanioideae, cyperaceae) from the amazon forest, Brazil. Acta Amazonica 2014;44(4):447–56.

[20] Heredia ULD, Duro-Garcia M, Soto A. Leaf morphology of progenies in Q. suber, Q. ilex, and their hybrids using multivariate and geometric morphometric analysis. iForest - Biogeosci Forestry 2018;(1):90–8. http://dx.doi.org/10.3832/ifor2577-010, URL https://iforest.sisef.org/contents/?id=ifor2577-010.

[21] Sileshi F, Galano T, Biri B. Plant disease diagnosis practical laboratory manual. 2016.

[22] Ks A, Sahayadhas A. Automatic rice leaf disease segmentation using image processing techniques. Int J Eng Technol(UAE) 2018;7:182–5.

[23] Gutierrez A, Ansuategi A, Susperregi L, Tubío C, Rankić I, Lenža L. A benchmarking of learning strategies for pest detection and identification on tomato plants for autonomous scouting robots using internal databases. J Sensors 2019;2019.

[24] Nguy-Robertson A, Peng Y, Arkebauer T, Scoby D, Schepers J, Gitelson A. Using a simple leaf color chart to estimate leaf and canopy chlorophyll a content in maize (zea mays). Commun Soil Sci Plant Anal 2015;46(21):2734–45. http://dx.doi.org/10.1080/00103624.2015.1093639.

[25] Intaravanne Y, Sumriddetchkajorn S. Android-based rice leaf color analyzer for estimating the needed amount of nitrogen fertilizer. Comput Electron Agric 2015;116:228–33. http://dx.doi.org/10.1016/j.compag.2015.07.005.

[26] Friedman JM, Hunt ER, Mutters RG. Assessment of leaf color chart observations for estimating maize chlorophyll content by analysis of digital photographs. Agron J 2016;108(2):822–9.

[27] Bauer J, Jarmer T, Schittenhelm S, Siegmann B, Aschenbruck N. Processing and filtering of leaf area index time series assessed by in-situ wireless sensor networks. Comput Electron Agric 2019;165:104867. http://dx.doi.org/10.1016/j.compag.2019.104867.

[28] da Silva LA, Bressan PO, Gonçalves DN, Freitas DM, Machado BB, Gonçalves WN. Estimating soybean leaf defoliation using convolutional neural networks and synthetic images. Comput Electron Agric 2019;156:360–8. http://dx.doi.org/10.1016/j.compag.2018.11.040.

[29] Easlon HM, Bloom AJ. Easy Leaf Area: Automated digital image analysis for rapid and accurate measurement of leaf area. Appl Plant Sci 2014;2(7).

[30] Zhang J, Huang Y, Pu R, Gonzalez-Moreno P, Yuan L, Wu K, et al. Monitoring plant diseases and pests through remote sensing technology: A review. Comput Electron Agric 2019;165:104943. http://dx.doi.org/10.1016/j.compag.2019.104943.

[31] Croft H, Chen J. Leaf pigment content. Ref Module Earth Syst Environ Sci 2017. http://dx.doi.org/10.1016/B978-0-12-409548-9.10547-0.

[32] Kvet J, Marshall J. Assessment of leaf area and other assimilating plant surfaces. 1971, Sestak, Z. Plant photosynthetic production.

[33] Kogan M, Turnipseed S, Shepard M, De Oliveira E, Borgo A. Pilot insect pest management program for soybean in southern Brazil. J Econ Entomol 1977;70(5):659–63.

[34] Santos J, Costa R, Silva D, Souza A, Moura F, Junior J, et al. Use of allometric models to estimate leaf area in hymenaea courbaril l. Theor Exper Plant Physiol 2016;28. http://dx.doi.org/10.1007/s40626-016-0072-8.
[35] Carvalho JOD, Toebe M, Tartaglia FL, Bandeira CT, Tambara AL. Leaf area estimation from linear measurements in different ages of Crotalaria juncea plants. Anais Acad Brasileira Ciencias 2017;89:1851–68. http://dx.doi.org/10.1590/0001-3765201720170077.
[36] LI-COR. LI-3000c area meter. 2023, URL https://www.licor.com/. [Accessed: 11 October 2023].
[37] ADC. AM350 portable leaf area meter. 2023, URL https://www.adc.co.uk. [Accessed: 11 October 2023].
[38] Carrasco-Benavides M, Mora M, Maldonado G, Olguín-Cáceres J, von Bennewitz E, Ortega-Farias S, et al. Assessment of an automated digital method to estimate leaf area index (LAI) in cherry trees. New Zealand J Crop Horticu Sci 2016. http://dx.doi.org/10.1080/01140671.2016.1207670.
[39] Liang W, Kirk KR, Greene JK. Estimation of soybean leaf area, edge, and defoliation using color image analysis. Comput Electron Agric 2018;150:41–51. http://dx.doi.org/10.1016/j.compag.2018.03.021.
[40] Silva M, Ribeiro S, Bianchi A, Oliveira R. An improved deep learning application for leaf shape reconstruction and damage estimation. In: Proceedings of the 23rd international conference on enterprise information systems - volume 1: ICEIS. SciTePress, INSTICC; 2021, p. 484–95. http://dx.doi.org/10.5220/0010444204840495.
[41] Corona G, Maciel-Castillo O, Morales-Castañeda J, Gonzalez A, Cuevas E. A new method to solve rotated template matching using metaheuristic algorithms and the structural similarity index. Math. Comput. Simul. 2023;206:130–46.
[42] Rusia MK, Singh DK. A comprehensive survey on techniques to handle face identity threats: challenges and opportunities. Multimedia Tools and Appl. 2023;82(2):1669–748.
[43] Feng C, Cao Z, Xiao Y, Fang Z, Zhou JT. Multi-spectral template matching based object detection in a few-shot learning manner. Inf. Sci. 2023;624:20–36.
[44] Oya N, Rusdi M, Fazlina Y, Sugianto S. Template matching method to determine oil palm trees. In: IOP Conference Series: Earth and Environmental Science. 1183, (1):IOP Publishing; 2023, p. 012077.
[45] Juwono FH, Wong W, Verma S, Shekhawat N, Lease BA, Apriono C. Machine learning for weed–plant discrimination in agriculture 5.0: An in-depth review. Artif. Intell. Agric. 2023.
[46] Bai Y, Zhang B, Xu N, Zhou J, Shi J, Diao Z. Vision-based navigation and guidance for agricultural autonomous vehicles and robots: A review. Comput. Electron. Agric. 2023;205:107584.
[47] Hughes DP, Salathé M. An open access repository of images on plant health to enable the development of mobile disease diagnostics through machine learning and crowdsourcing. 2015, arXiv, arXiv:1511.08060.
[48] Mohanty SP, Hughes DP, Salathé M. Using deep learning for image-based plant disease detection. Front Plant Sci 2016;7:1419. http://dx.doi.org/10.3389/fpls.2016.01419.
[49] Hu G, Wei K, Zhang Y, Bao W, Liang D. Estimation of tea leaf blight severity in natural scene images. Precis Agric 2021;22(4):1239–62.
[50] Amirkhani D, Bastanfard A. An objective method to evaluate exemplar-based inpainted images quality using jaccard index. Multimedia Tools Appl 2021;80(17):26199–212.
[51] Sadeghi-Tehran P, Virlet N, Sabermanesh K, Hawkesford MJ. Multi-feature machine learning model for automatic segmentation of green fractional vegetation cover for high-throughput field phenotyping. Plant Methods 2017;13(1):103.
[52] Soares FAAMN, Flôres EL, Cabacinha CD, Carrijo GA, Veiga ACP. Recursive diameter prediction and volume calculation of eucalyptus trees using multilayer perceptron networks. Comput Electron Agric 2011;78(1):19–27.
[53] Bradshaw JD, Rice ME, Hill JH. Digital analysis of leaf surface area: effects of shape, resolution, and size. J Kansas Entomol Soc 2007;80(4):339–47.
[54] Maloof JN, Nozue K, Mumbach MR, Palmer CM. LeafJ: an ImageJ plugin for semi-automated leaf shape measurement. JoVE (J Visual Exper) 2013;(71):e50028.
[55] Keramatlou I, Sharifani M, Sabouri H, Alizadeh M, Kamkar B. A simple linear model for leaf area estimation in Persian walnut (juglans regia l.). Sci Hortic 2015;184:36–9.
[56] Kaur G, Din S, Brar AS, Singh D. Scanner image analysis to estimate leaf area. Int J Comput Appl 2014;107(3).